CONF-830301--18

EFFECT OF NONUNIFORM INLET AIR FLOW ON AIR-COOLED HEAT-EXCHANGER PERFORMANCE

by

Alan I. Soler, Ph.D.
Professor of Mechanical Engineering and Applied Mechanics
University of Pennsylvania, Philadelphia, Pennsylvania

Krishna P. Singh, Ph.D.
Vice President Engineering

Teik-Lee Ng, Project Engineer
Joseph Oat Corporation, Camden, New Jersey

DE83 016363

ABSTRACT

Blowers used to propel air across tube bundles generate a non-uniform flow field due to their construction details. Reduction in the heat transfer rate due to such non-uniformity is generally recognized in the commercial air cooler industry. However, the common antidote is to add sufficient heat transfer surface area to compensate for such losses. Such an approach is unacceptable in those applications where the outlet temperature of the hot (in-tube) medium is sought to be controlled precisely.

A formalism to evaluate heat transfer degradation due to non-uniform airflow has been developed. Certain symmetry relations for cross flow heat exchangers, heretofore unavailable in the open literature, have been derived.

The solution presented here was developed to model a 4 tube pass air blast heat exchanger for the Clinch River Breeder reactor project. This case is utilized to show how this method can be used as a design tool to select the most suitable blower construction for a particular application. A numerical example is used to illustrate the salient points of the solution.

NOMENCLATURE(any consistent set of units may be used)

A:	Heat transfer area
A_b:	Duct side surface area of bare tube/unit length of tube
A_i:	Inside surface area of tube/unit length of tube
A_o:	Total outside surface area of finned tube/unit length of tube
A_f:	Total fin area/unit length of tube
b,c:	Specified constants (eq. 10)
c_{p_s}, c_{p_t}:	Specific heat of shellside, tubeside fluid. (The shellside fluid is air)
d_i, d_o:	Tube I.D., O.D.
h_s, h_t:	Shell-side, tubeside heat transfer coefficient
I:	Integral function (eq. 9)
k_w:	Thermal conductivity of tube wall
ℓ:	Fin height
L:	Tube length
m_s, m_t:	Shell side, tubeside mass flowrate
P:	Equivalent perimeter of the tube
Q:	Heat duty
r:	Bare tube radius (eq. 24)
Re_s, Re_t:	Reynolds number of shell side, tubeside fluid
R_w:	Tube wall resistance
s:	Spacing between adjacent fins (or pitch)
t:	Fin thickness
t_i:	Tube-side inlet temperature in the control volume (Fig. 4)
t_o:	Tube-side outlet temperature in the control volume (Fig. 4)
T_s:	Shell-side fluid temperature
T_t:	Tube-side temperature
U:	Overall heat transfer coefficient
x:	Coordinate along tube axis (Fig. 2)
Δ:	Determinant (eq. 19)
ΔA:	Incremental surface area of heat transfer
ΔQ:	Heat transfer rate from a tube segment of length Δx
ΔT_t:	Incremental change in tube fluid temperature (Fig. 1)
α_{jk}, β_{jk}:	Defined parameters (eqs. 12, 16)
γ:	Defined parameter (eq. 6a)
η:	Fin efficiency (eq. 24)
η_w:	Weighted fin efficiency (eq. 23)
θ:	Difference between tube fluid temperature and air inlet temperature (eq. 6b)
$\phi(x)$:	Mass flowrate of air per unit of tube length
m,ψ:	Parameters used in eq. (24) and defined in reference [5]
μ:	Numerical value, $0<\mu\leq 1$ (eq. 26)

Subscripts

i:	Value at inlet
o:	Value at outlet
j:	Vertical plane divider number (Fig. 3)
k:	Stratum number in the discretized grid (Fig. 3)

DISCLAIMER

jk: Value of the quantity in the control volume bounded by vertical planes j and (j+1); and strata k and (k+1)
u: Denotes uniform
m: Denotes maximum

INTRODUCTION:

It is well known that air exiting commercial blowers have a non-uniform velocity distribution. This non-uniformity of flow is generally not considered a problem in blower applications (both axial flow and centrifugal type) to air coolers, since any loss in the cooler overall heat transfer rate due to air velocity maldistribution is completely overshadowed by other design uncertainties, e.g. fouling rate of the tube surfaces, heat transfer properties of the in-tube fluid, etc. Because of the larger effect of other uncertainties in many commercial applications, scientific interest in the effect of air maldistribution on derating of air coolers has been minimal. Recently, this situation has undergone some change because of the introduction of cross flow air coolers in the nuclear power industry. Air coolers have been employed to dissipate heat produced by the experimental reactors at the "fast flux test facility" at Hanford, Washington [1]. Recently, forced draft air blast heat exchangers have been designed for use in the Clinch River Breeder Reactor project. In these applications, the tubes contain liquid sodium or sodium-potassium eutectic; these fluids have a very high surface heat transfer coefficient which results in the air side heat transfer coefficient controlling the heat transfer rate. Therefore, variations in the air side heat transfer coefficient values could materially affect overall heat transport. Accurate determination of the heat transfer rate in cross flow air cooled liquid metal heat exchangers is of some importance to ensure that overcooling does not cause in-tube freezing; or overstress in the tubes due to differential thermal expansion [2].

In this paper, we examine the effect of lengthwise variation of the overall heat transfer coefficient, U (due to inlet air maldistribution) on the heat duty. We derive analytical expressions for an idealized one tube pass cross flow system in order to discern certain symmetry relations which have heretofore not been reported in the open literature.

Next a numerical scheme to determine the temperature field in a multiple pass-cross flow heat exchanger is devised. This method is applied to study the performance deterioration of a four tube pass cross flow heat exchanger due to airside maldistribution of flow. Similar studies on the effects of tube side maldistribution have been performed by McDonald and Eng [3].

The purpose of this research is twofold: 1) we seek to develop the necessary theory to study the effect of inlet air maldistribution on heat duty; and 2) we seek to determine typical results for realistic units.

2. Analysis of a Single Tube Pass

Referring to Fig. 1, conservation of heat energy over a tube element on length Δx and heat transfer surface area ΔA gives:

$$\Delta Q = -\dot{m}_t C_{pt} \Delta T_t = \phi(x)\Delta x\, C_{ps}(T_{so} - T_{si}) \qquad (1)$$

where $\phi(x)$ is the shellside mass flowrate of air per unit length of tube.

Similarly,

$$\Delta Q = U\Delta A\left\{(T_{avg})_{tube} - T_{avg})_{shell}\right\} \qquad (2)$$

or

$$\Delta Q = \frac{U\Delta A}{2}\left\{2T_t + \Delta T_t - T_{si} - T_{so}\right\}$$

Let $\Delta A = P\Delta x$ (3)

where P is the equivalent perimeter of the tube (including any effect of fins). From Eqs. (1) - (3), we have in the limit as $\Delta x \to 0$

$$T_{so} = \frac{UPT_t - UP\,T_{si}/2 + \phi(x)\, C_{ps}T_{si}}{(UP/2 + \phi(x)C_{ps})} \qquad (4)$$

Eliminating T_{so} from eq. (1), yields

$$\frac{dT_t}{dx} = \frac{-\phi(x)\, C_{ps}\, UP(T_t - T_{si})}{\dot{m}_t\, C_{pt}(\phi(x)\, C_{ps} + .5\, UP)} \qquad (5)$$

We define $\gamma(x)$, $\theta(x)$ by relations

$$\gamma(x) = \frac{\phi C_{ps}\, UP}{\dot{m}_t C_{pt}(\phi C_{ps} + .5UP)} \qquad (6a)$$

$$\theta(x) = T_t(x) - T_{si} \qquad (6b)$$

Then, eq. (5) reduces to

$$\frac{d\theta}{dx} = -\gamma(x)\theta \;;\; \theta(x) = \theta|_{x=0}\, e^{-\int\gamma(x)dx}$$

Therefore, T_t is given as

$$T_t(x) = T_{si} + (T_{ti} - T_{si})\; e^{-\int_0^x \gamma(y)dy} \qquad (7)$$

The total amount ofheat transferred is calculated as

$$Q = \dot{m}_t C_{pt}\,(T_{ti} - T_{to})$$

where $T_{to} = T_t|_{x=L}$ from Eq. (7). The final result for Q for the single tube, is

$$Q = \dot{m}_t C_{pt}(T_{ti} - T_{si})\left[1 - e^{-\int_0^L \gamma(y)dy}\right] \qquad (8)$$

The above equation implies the plausible result that as L approaches infinity, the tubeside outlet temperature will approach the shellside (air) inlet temperature.

The significant result of this simple calculation is that for a given set of inlet temperatures and tube surface, a change in the heat duty Q can only by induced by a change in the integral I, given by

$$I = \int_0^L \gamma(x)dx \qquad (9)$$

Inspection of the expression for $\gamma(x)$ (eq. 6a) indicates that there are two quantities ϕ and U which are functions of x. Since the overall heat transfer coefficient U is actually an explicit function of the flowrate per unit length $\phi(x)$, γ can be cast as an explicit function of ϕ alone. Therefore, the integral I depends ultimately on $\phi(x)$.

$$I = \int_0^L \frac{\phi f(\phi)}{[bf(\phi) + c\phi]}\, dx \qquad (10)$$

where $f(\phi) = U$, $b = .5M_tC_{pt}/C_{ps}$, and $c = M_tC_{pt}/P$. It is easily shown that if ϕ, ϕ^* are functions such that $\phi(x) = \phi^*(L - x)$, then

$$I(\phi) = I(\phi^*)$$

Thus, the total heat duty for any air flow profile is equal to that of its mirror image about the central plane $x = L/2$. For example, the heat duty due to the two triangular air flow profiles shown in Figure 2 will be equal.

Finally, the air mass flow rate profile function $\phi(x)$ which will maximize Q for a given tube surface and total air flow rate, m_s, can be obtained by seeking the function $\phi(x)$ which maximizes the integral subject to the constraint that the total air flow rate remains as given for the unit. The necessary criterion for the optimal function $\phi(x)$ is found by using Euler's equation in variational calculus [ref. 4, p. 355], and generally leads to a nonlinear ordinary differential equation for the optimum distribution of air velocity $\phi(x)$ which maximizes the heat duty Q.

Extension of the above methodology to practical multiple tube pass configurations is possible. However, it is far more expedient to construct a numerical solution which can be readily computerized. We will now proceed to develop such a solution bearing in mind that in the limit it should produce results in agreement with the idealized single tube system just discussed.

3. Multiple Tube Pass-Cross Flow Construction

Let us consider a multiple tube pass configuration, such as the one shown in Figure 3. As shown in Figure 3, the tube side fluid remains unmixed, and the shell side fluid (air) is also assumed to remain unmixed. Figure 3 shows three rows of tubes in each pass and a total of 4 tube passes. This is for illustrative purposes only. The analysis is not limited to a specific number of tube passes, or a specific number of tube rows per pass. Mixing of the tubeside fluid at the extremity of each pass is also permitted. All quantities are assumed to be uniform along the lateral dimension (into the plane of paper in Fig. 3). For the purpose of numerical analysis, the tube rows divide the air space into k + 1 strata where k is the total number of tube rows. Thus the incipient air is labeled as stratum 1, and the exiting air is labeled as stratum 13 in Fig. 3. The air stratum is denoted by the subscript k. Similarly, the longitudinal span of tube matrix space is divided into N chambers by vertical planes shown by dotted lines in Fig. 3. These vertical planes are labeled $j = 1,\ldots,(N+1)$ as shown in Fig. 3. N is selected sufficiently large such that the air mass in the space in a chamber bounded by two adjacent strata can be assumed to be at a uniform temperature. The choice of N may be established by performing convergence studies for a particular unit configuration. Both airside quantities m_s, c_{ps}, T_s and tubeside quantities m_t, c_{pt}, T_t are functions of location (i.e., position parameters j and/or k). The solution algorithm is developed by examination of the tube segment in row k, bounded by vertical planes j and (j+1). Figure 4 shows mass flow rates and terminal temperatures. Tubeside inlet and outlet temperatures are indicated as t_i and t_o, respectively. We note, for example, that for $k = 1,2,3$, $t_i = T_{t(j+1)}$ and $t_o = T_{t(j)}$, whereas for $k = 4,5$ and 6, $t_i = T_{t(j)}$ and $t_o = T_{t(j+1)}$.

A heat balance with tubeside fluid yields:

$$m_{tk}\, C_{pt,jk}(t_i - t_o) = (UA)_{jk}\left[\frac{t_i + t_o}{2} - \frac{T_{s(k+1)} + T_{sk}}{2}\right] \qquad (11)$$

Note that m_t varies only with stratum since each tube may have a different flowrate.

Let $$\alpha_{jk} = (UA)_{jk}/(2m_{tk}\, c_{pt,jk}) \qquad (12)$$

Then we have

$$(1 - \alpha_{jk})\, t_i + \alpha_{jk}T_{sk} - t_o(1 + \alpha_{jk}) + \alpha_{jk}T_{s(k+1)} = 0 \qquad (13)$$

Similarly, a heat balance with the air stream, noting that m_s varies only with the location j, yields

$$m_{sj}C_{ps,jk}\,(T_{s(k+1)} - T_{sk}) = (UA)_{jk}\left[\frac{t_i + t_o}{2} - \frac{(T_{s(k+1)} + T_{sk})}{2}\right] \qquad (14)$$

or

$$(\beta_{jk} - 1)T_{sk} - \beta_{jk}\, t_i + (1 + \beta_{jk})\, T_{s(k+1)} - \beta_{jk}t_o = 0 \qquad (15)$$

where

$$\beta_{jk} = (UA)_{jk}/(2m_{sj}C_{ps,jk}) \qquad (16)$$

Simultaneous equations (13) and (15) are solved for t_i and $T_{s\,(k+1)}$ and yield

$$t_i = [t_o(1 + \alpha_{jk} + \beta_{jk}) - 2\alpha_{jk} T_{sk}]/\Delta \quad (17)$$

$$T_{s(k+1)} = [2t_o \beta_{jk} + T_{sk} (1 - \alpha_{jk} - \beta_{jk})]/\Delta \quad (18)$$

$$\text{where } \Delta = 1 + \beta_{jk} - \alpha_{jk} \quad (19)$$

The solution procedure can be started at $j = k = 1$ where the tube outlet temperature $T_{t,11} = t_o$, and air inlet temperature $T_{s,11}$ are known. Equation (17) gives the value of t_i which, in turn, defines the outlet temperature for the region $j = 2$, $k = 1$. The solution is continued for $j = 1,2,\ldots,$ through to $j = N$. The air inlet temperature profile is now known from equation (18) for the second stratum ($k = 2$), and hence similar computations are performed for row #2, etc. For passes #3 and #1, the computations must then proceed from right to left. In this manner, the temperatures of the tubeside fluid and air at all discretized control volume locations are determined.

In the following section, a numerical example is utilized to illustrate the use of the above solution scheme to assess the effect of air flow maldistribution on the heat exchanger performance.

4. Numerical Example

Let us consider the heat transfer from a liquid-metal eutectic of sodium potassium, flowing inside tubes, to air flowing upwards through a 4-pass arrangement of finned tubes. Fin and tubing are both stainless steel. Each pass is arranged in three rows of tubes in a staggered array. Figure 3 is the schematic detail of the arrangement. The tubes are 1-1/4" O.D. (3.175 cm.) and 13 BWG with 5/8" high x .075" (1.5875 cm. x .1905 cm.) thick helical fins attached to the tube through high frequency resistance welding. The helical pitch is .147" (.3734 cm.)

Correlations by Briggs and Young [5] for airside film coefficient (Eq. 20) and by Fraas [6] for the tube-side coefficient (Eq. 21) are used.

$$Nu_s = .134\, Re_s^{.681}\, Pr_s^{.333}\, (s/\ell)^{.2} (s/t)^{.1134} \quad (20)$$

$$Nu_t = 7 + .025\, (Re_t\, Pr_t)^{.8} \quad (21)$$

The overall film coefficient can be calculated by

$$U = \left[\frac{1}{\eta_w h_s} + \frac{A_o}{A_b} R_w + \frac{A_o}{A_i h_t}\right]^{-1} \quad (22)$$

where the weighted fin efficiency is

$$\eta_w = 1 - \frac{A_f}{A_o}(1 - \eta) \quad (23)$$

The fin efficiency is determined by Schmidt's [7] relation

$$\eta = \frac{\tanh(m r\psi)}{m r \psi} \quad (24)$$

Finally the wall resistance term in eq. (22) is given by

$$R_w = \frac{d_o \ln(d_o/d_i)}{2 K_w} \quad (25)$$

In this example eq. (21) yields tube-side coefficients (h_t) in the order of 2000 Btu/hr-sq ft °F (40.88 x 10^3 J/hr-sq.m.-°C). The airside coefficient (h_s) determined from eq. (20) is only 15 Btu/hr-sq ft -°F (306.5 J/hr-sqm. °C). Thus it is clear from eq. (22) that the overall coefficient is governed by the airside coefficient. We also note that h_s is strongly dependent on the Reynolds number (eq. 20) which is a function of flow velocity. Thus the functional relationship between the overall heat transfer coefficient and the flow velocity is available. Computer program "AIRCROSS" is written to solve the heat transfer problem using the foregoing.

A simple linearly maldistributed airflow profile as shown in Fig. 4 is used. The air mass flowrate function $\phi(x)$ can be represented by

$$\phi(x) = \left[1 - \frac{x}{L}(1 - \mu)\right] \phi_m \quad (26)$$

The image of this profile about the central plane across the tube axis is given by

$$\phi^*(x) = \left[1 - (1 - \frac{x}{L})(1 - \mu)\right]\phi_m \quad (27)$$

If we have a constant shell-side average lineal air mass flow rate ϕ_u entering the heat exchanger then

$$\phi_u = \frac{1}{L}\int_0^L \phi(x)dx \quad (28)$$

Equations (26)-(28) yield

$$\phi_m = 2\phi_u/(1 + \mu) \quad (29)$$

Initially, the solution is carried out for a uniform airflow profile equal to ϕ_u over the entire length of the heat exchanger. Subsequent runs are made using the incoming air profiles described by eqs. (26) and (27) for values of μ equal to 0.5, 0.25, 0.1 and 0.01.

The following additional input data is utilized:

Total surface area: 5460 ft² (524 m²)
Tubeside mass flow rate: 165000 lb/hr(74843kg/hr)
Shellside (air) volume flowrate: 50000 cfm at 100°F (1416 m³/min)
Tubeside inlet temperature: 980°F (526.67°C)
Airside inlet temperature: 100°F (37.78°C)
A_o = 428.8 in²/ft (.906 m²/m); A_b = 47.12 in²/ft (.0997 m²/m.)
4 tube pass; airside fluid unmixed
The average tubeside heat transfer coefficient is computed to be 2037 Btu/hr-ft² °F (41.64 x 10^3 J/hr- sq.m.°C)
The tube wall resistance is 7.156 x 10^{-4} (BTU/hr-ft°F)$^{-1}$ (.35 x 10^{-4}(J/hr-sq.m.°C)$^{-1}$)

Using the computer code, the heat duties for various cases are determined; the effect of air maldistribution is shown in Table 1.

Our numerical studies show that for a given value of μ the percentage degradation is identical for the maldistributed airflow and its mirror image. This conclusion is consonant with the mathematical deduction made for single tube pass configurations in section 2. Additional computations, not presented here, have been carried out to test the configuration for heat duty degradation under a wide variety of air flow distribution functions. Under some extreme flow profiles, % degradation values as high as 9 have been computed; it is likely, however, that these extreme profiles would not be observed in a practical situation.

CONCLUSIONS

Constitutive equations for cross flow in single tube pass heat transfer problems are integrated for an arbitrary inlet air mass flow profile. It is shown that the total unit heat transfer rates obtained for a given maldistributed air profile and its mirror image are equal. Subsequent numerical integration of the heat transfer equations for multiple pass designs indicate that such symmetry relations hold for multiple pass configurations as well.

The method for numerical quadrature of heat transfer equations presented in this paper enable rapid evaluation of the effects of air mass flow maldistribution. Our studies show that the derating of the overall heat duty is quite small, even for severely non-uniform flows. Thus, in a typical situation, non-uniform air flow alone would not cause significant deterioration in heat transfer. However, in concert with other deviations from the ideal, such an imperfect fin-to-tube bond, tubeside maldistribution, air bypass, etc., a significant derating of a unit may occur. The procedure evolved herein enables the user to ascertain quantitative results for any set of input data.

REFERENCES

[1] D.C. Bastow and E.C. Seber, "Considerations in Designing High Temperature Dump Heat Exchangers", ASME Paper 76-JPGC-NE-7.

[2] Singh, K.P. and M. Holtz, "On Thermal Expansion Induced Stresses in U-Bends of Shell-and-Tube Heat Exchangers", Journal of Engrg. for Power, Trans ASME, Vol. 101, No. 3, Oct. 1979.

[3] McDonald, J.S. and K.Y. Eng, "Tube Side Flow Distribution Effects on Heat Exchanger Performance", Chemical Engineering Progress Symposium Series 41, vol. 49, pp. 11-17 (1963).

[4] Hildebrand, F.B., Advanced Calculus for Applications, Prentice-Hall (1962).

[5] Briggs, D.E., E.H. Young, "Convective Heat Transfer and Pressure Drop of Air Flowing across Triangular Pitch Banks of Finned Tubes", Chem. Eng. Prog. Sym. Ser., Vol. 59, no. 41, pp. 1-10, 1963.

[6] Fraas, Arthur, et al., Heat Exchanger Design, Wiley 1965, p. 51.

[7] Schmidt, T.E., "la Production Calorifique des Surfaces Munies D'ailettes", Annexe Du Bulletin De L'Institut International Du Froid, Annexe G-5, 1945-46.

Table 1

μ	0.5	0.25	0.1	0.01
% degradation[+]	.4	1.3	2.7	4.4

[+]Degradation of heat duty relative to the case of uniform flow

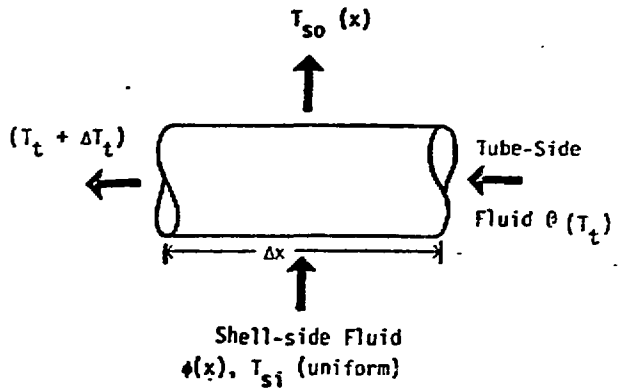

Fig. 1 Heat Transfer for a Tube Element

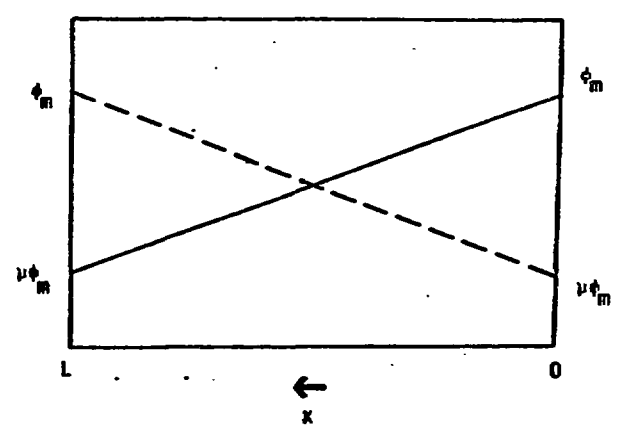

Fig. 2 Lineal Air Mass Flow Profile

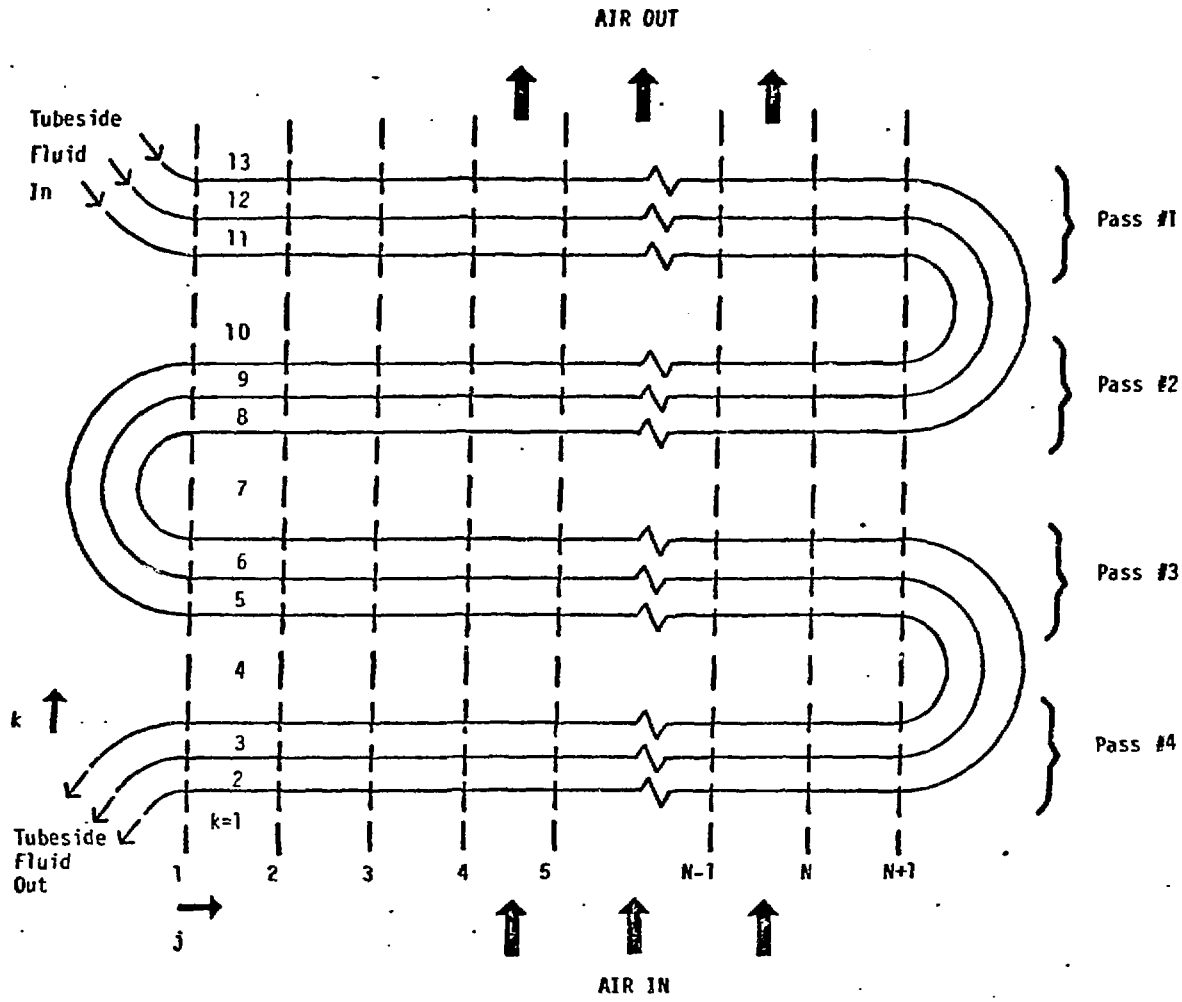

Fig. 3 Discretized Heat Transfer Model

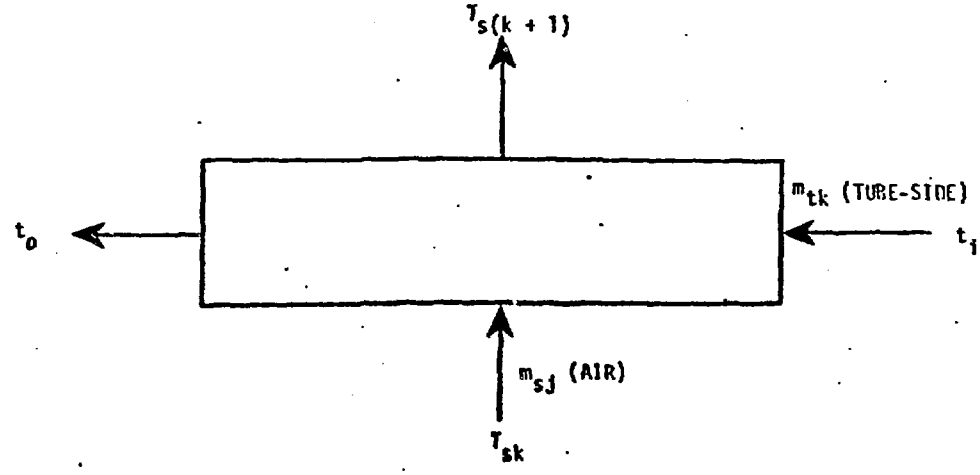

Fig. 4 Heat Transfer in Control Volume (j,k)